Inorganic Chemistry

Article

pubs.acs.org/IC

Redox Potential and Electronic Structure Effects of Proximal Nonredox Active Cations in Cobalt Schiff Base Complexes

Alexander H. Reath, Joseph W. Ziller, Charlene Tsay, Austin J. Ryan, and Jenny Y. Yang*

Department of Chemistry, University of California, Irvine, California 92697, United States

Supporting Information

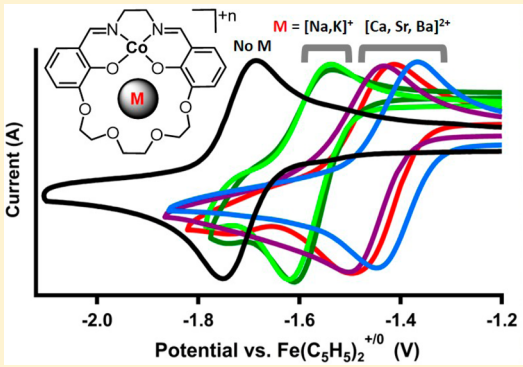

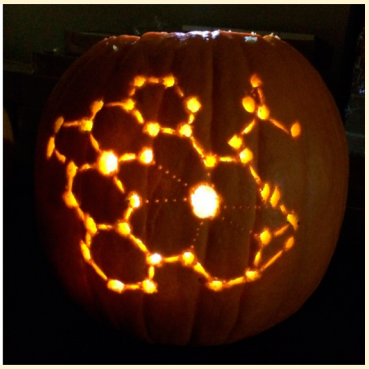

ABSTRACT: Redox inactive Lewis acidic cations are thought to facilitate the reactivity of metalloenzymes and their synthetic analogues by tuning the redox potential and electronic structure of the redox active site. To explore and quantify this effect, we report the synthesis and characterization of a series of tetradentate Schiff base ligands appended with a crown-like cavity incorporating a series of alkali and alkaline earth Lewis acidic cations (**1M**, where M = Na^+, K^+, Ca^{2+}, Sr^{2+}, and Ba^{2+}) and their corresponding Co(II) complexes (**2M**). Cyclic voltammetry of the **2M** complexes revealed that the Co(II/I) redox potentials are 130 mV more positive for M = Na^+ and K^+ and 230−270 mV more positive for M = Ca^{2+}, Sr^{2+}, and Ba^{2+}compared to Co(salen−OMe) (salen−OMe = *N*,*N*′-bis(3-methoxysalicylidene)-1,2-diaminoethane), which lacks a proximal cation. The Co(II/I) redox potentials for the dicationic compounds also correlate with the ionic size and Lewis acidity of the alkaline metal. Electronic absorption and infrared spectra indicate that the Lewis acid cations have a minor effect on the electronic structure of the Co(II) ion, which suggests the shifts in redox potential are primarily a result of electrostatic effects due to the cationic charge.

INTRODUCTION

Nonredox active Lewis acidic metal cations play a key role in a diverse set of biological and synthetic transition metal complexes that mediate redox activity. In biological systems, the Ca^{2+} ion found in the oxygen evolution complex (OEC) in Photosystem II is critical for water oxidation activity.[1] In synthetic transition metal complexes, the presence of Lewis acidic metals are known to promote C−H oxidation,[2] oxygen atom transfer,[3] olefin hydrogenation,[4] and oxygen reduction[5] reactions, as well as facilitate electron transfer reactions.[6]

One of the proposed roles that proximal redox inactive metal cations play in promoting reactivity is tuning the redox potential of the reaction site. Redox tuning by incorporation of redox inactive cations has been reported in several synthetic systems including mono-[4,7] and multimetallic manganese[8] and triiron[9] clusters incorporating Lewis acid cations through oxo-bridges. Additionally, pendant crown ethers encapsulating alkali or alkaline earth metals have been appended onto molybdenum,[10] ferrocene,[11] and iron pyridinediimine[12] complexes.

The shifts in the reversible redox potential denote a change in the absolute energy of the molecular orbital participating in electron transfer. We were interested in investigating how the Lewis acid cations engender this change. An inductive effect due to a modification of the ligand field would result in changes to the electronic structure (or molecular orbitals) of the redox active cation. In contrast, an electrostatic effect would uniformly shift the molecular orbitals on the redox active metal due to the electric field potential of the proximal cation.

To elucidate the source of the change in redox potential due to adjacent Lewis acidic cations, we synthesized a series of cobalt(II) Schiff base complexes with an appended crown functionality containing a series of alkali and alkaline earth metal cations (**2M** in Chart 1, M = Na^+, K^+, Ca^{2+}, Sr^{2+}, and Ba^{2+}). These compounds are well-suited to investigate the difference between inductive and electrostatic effects. The ligand provides a cavity similar in size to 18-crown-6, and can enclose a variety of ions with minimal effect on the coordination geometry of the Co(II) ion. Within this framework, the Co(II/I) couple is reversible, allowing a direct handle on changes in redox potential. The similar ligand environments permit facile comparisons in electronic structure

Received: February 2, 2017
Published: February 27, 2017

DOI: 10.1021/acs.inorgchem.6b03098
Inorg. Chem. 2017, 56, 3713−3718

Chart 1

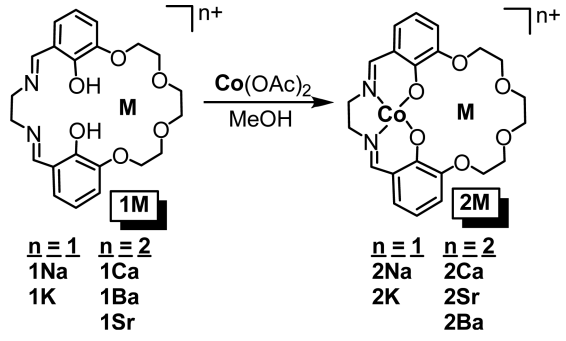

of the Co(II) ions due to the Lewis acid. The localization of the redox event at a single metal center instead of a cluster permits a more accurate calculation of an electrostatic effect. The shared phenoxide ligand between the Co(II) and Lewis acid cation is also relevant to the interaction between Mn and Ca^{2+} in the OEC. Additionally, redox inactive metal cations bound through μ-oxo ligands are known to play a role in synthetic cobalt oxide water oxidation catalysts.[13]

RESULTS AND DISCUSSION

Synthesis. The Schiff base ligands **1M** (Chart 1) contain an alkali or alkaline earth metal cation in an appended ether pocket. Using a modified literature procedure,[14] **1Ba(OTF)$_2$** was synthesized by templating an ether-linked dialdehyde with $Ba(OTf)_2$, followed by condensation with ethylenediamine. **1Na(OTf)**, **1K(OTf)**, **1Ca(OTf)$_2$**, and **1Sr(OTf)$_2$** were synthesized in a similar fashion using the appropriate metal triflate salt and purified by recrystallization. The **1M** series was characterized by high-resolution mass spectrometry (HRMS) and ^{1}H and ^{13}C NMR spectroscopy, which are shown in the Supporting Information (Figures S1–S10). There is a linear relationship between the size of the nonredox active cation[15] and chemical shift of the phenolic protons in the ^{1}H NMR spectra, illustrated in Figure S11.

The ionic radius of the templating alkali or alkaline earth cation has a significant effect on the synthetic accessibility of the **1M** ligand series. **1K(OTf)** is synthesized in the highest yield, while the yields for the other reported ligands decrease with larger or smaller cation sizes. The use of even smaller cations (Li^+ or Mg^{2+}) as a template did not result in the desired product. For ions too large to fit in the crown ether cavity (ionic radii >150 pm), such as Rb^+ and Cs^+, mass spectrometry suggests the formation of aggregates, presumably in stacked, sandwich-like structures with the metal ions coordinated between crown ether macrocycles (see Figure S12 for MS from the reaction with Cs(OTf)). Sandwich complexes of this type have been observed for similar complexes containing crown ether structures and large cations.[16] We also attempted to synthesize **1M** using the trications Al^{3+}, Ga^{3+}, In^{3+}, Y^{3+}, and La^{3+} but were unable to isolate the desired product using the procedure descibed above.

The Co(II) complexes **2M** (where M = Na^+, K^+, Ca^{2+}, Sr^{2+}, and Ba^{2+}) were synthesized by refluxing the corresponding **1M** ligand with one equivalent of $Co(OAc)_2$ in methanol, followed

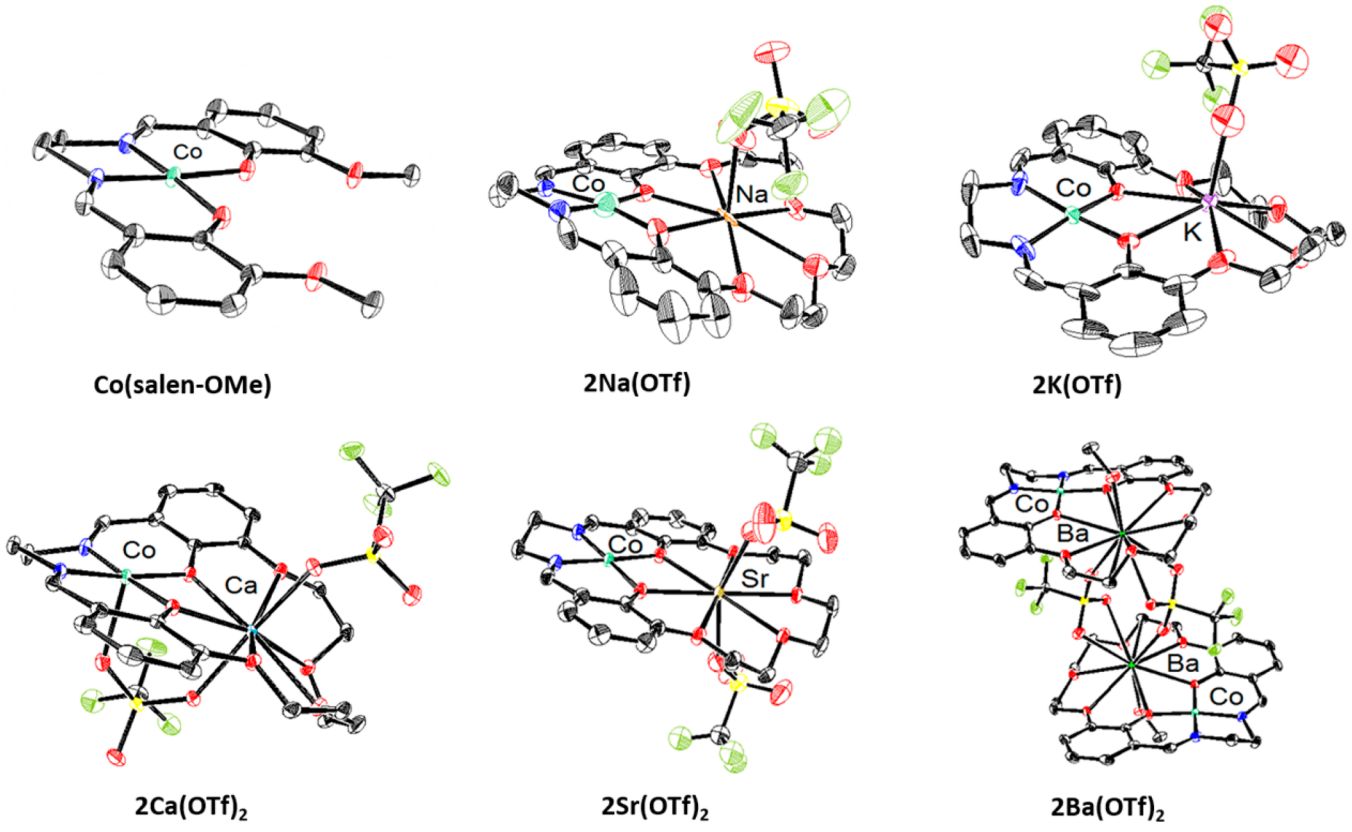

Figure 1. Solid-state structures of Co(salen–OMe), 2Na(OTf), 2K(OTf), 2Ca(OTf)$_2$, 2Sr(OTf)$_2$, and 2Ba(OTf)$_2$. Thermal ellipsoids are drawn to 50% probability. Hydrogen atoms and outer-sphere anions and solvent molecules have been omitted for clarity. For Co(salen–OMe) and 2Sr(OTf)$_2$, only one molecule of two in the asymmetric unit cell is shown. For 2K(OTf), 2Na(OTf), and 2Sr(OTf)$_2$, only the major position of a disordered system is displayed.

DOI: 10.1021/acs.inorgchem.6b03098
Inorg. Chem. 2017, 56, 3713–3718

Table 1. Summary of Structural, Spectroscopic, and Electrochemical Data for Co(salen−OMe) and 2M Complexes

complex	$E_{1/2}$[a] Co(II/I) (V)	ΔE[b] (V)	calc. ΔE[c] (V)	pK_a of M(OH$_2$) (aq.)	Co···M (Å)	Co(II)[f] ion (τ_4)	ν(C═N) (cm^{-1})	λ(d→d) (nm)	ε (M^{-1}cm^{-1})
Co(salen−OMe)	−1.71					0.0303	1535	480, 555	2700, 790
2K(OTf)	−1.58	0.13	0.11	16.25[d]	3.6694(1)	0.1148	1544	545	767
2Na(OTf)	−1.58	0.13	0.12	14.77[e]	3.338(5)	0.0295	1546	545	634
2Ba(OTf)$_2$	−1.48	0.23	0.21	13.36[e]	3.7045(2)	0.1113	1548	530	979
2Sr(OTf)$_2$	−1.44	0.27	0.22	13.18[e]	3.6078(4)	0.0622	1552	530	1012
2Ca(OTf)$_2$	−1.41	0.30	0.23	12.60[e]	3.3578(4)	0.0692	1557	530	881

[a]Reduction potentials in dimethylformamide referenced to ferrocene/ferrocenium. [b]Difference between the reduction potential of **2M** and Co(salen−OMe). [c]Calculated electric field potential on Co(II) due to M in **2M** complexes using eq 1. [d]Calculated through vapor pressure measurements of an aqueous solution (ref 21a). [e]Measured electrometrically in cells containing Ag/AgCl with hydrogen electrodes (ref 21b). [f]τ_4 value describing the coordination geometry around the Co(II) ions, where τ_4 = 1 for a tetrahedral geometry, and τ_4 = 0 for a square planar geometry

by removal of solvent and acetic acid *in vacuo*. The identities of the compounds were confirmed using mass spectrometry and single crystal X-ray diffraction analysis, and the purities by elemental analysis. Co(salen−OMe) (salen−OMe = *N*,*N*′-bis(3-methoxysalicylidene)-1,2-diaminoethane) was prepared for comparison with the **2M** complexes. Salen−OMe was synthesized according to a literature procedure,[17] and metalation with Co(OAc)$_2$ was based on a preparation of Co(*N*,*N*′-ethylenebis(salicylimine)).[18]

Structural Studies. Single crystals suitable for X-ray diffraction were grown by diffusion of diethyl ether into methanol solutions of the respective compounds. The solid-state structures for the **2M** triflate salts and Co(salen−OMe) are shown in Figure 1 (The X-ray crystallographic data for **2Na(OTf)** and **2K(OTf)** had significant disorder. Higher quality structures of the analogous tetrafluoroborate salts for **2Na(BF$_4$)** and **2K(BF$_4$)** are provided in the SI.

In all of the heterobimetallic complexes, the counteranion(s) are bound to the M cation. In the case of **2Ba(OTf)$_2$**, a molecule of methanol is coordinated to the Ba^{2+} cation along with two triflate anions, which form a symmetric bridge to another **2Ba(OTf)$_2$** complex. The mass spectrum does not contain peaks consistent with the dimer, suggesting that this species only exists in the solid-state.

Each complex contains a minimally distorted square planar cobalt with the group I or II cation occupying the crown ether cavity. The τ_4 values[19] describing the coordination around the Co(II) ions are listed in Table 1 and confirm similar coordination environments. The distances between the Co(II) ion and M cations are also listed in Table 1.

Electrochemistry. Cyclic voltammetry of Co(salen−OMe) in dimethylformamide displays a reversible reduction at −1.72 V versus ferrocene/ferrocenium (Figure 2, black trace), consistent with literature values[20] for a Co(II/I) redox couple. In comparison, the corresponding reductions for **2M** are observed at more positive potentials, as shown in Figure 2 (colored traces) and listed in Table 1. The Co(II/I) redox potential for the monocations is 130 mV more positive than Co(salen−OMe), while the Co(II/I) potential for the complexes with dications are 230−300 mV more positive than Co(salen−OMe). The differences in redox potential for the dicationic complexes also correlate with the Lewis acidity[21] of the Group II metal cations, shown in Figure 3, similar to the effect observed by metalloclusters incorporating redox inactive cations.[8,9] To ensure that there was no significant dissociation of M upon reduction, up to 10 equiv of Na^+, Ca^{2+}, and Ba^{2+} triflate salts were added to the respective **2M** solutions. Only

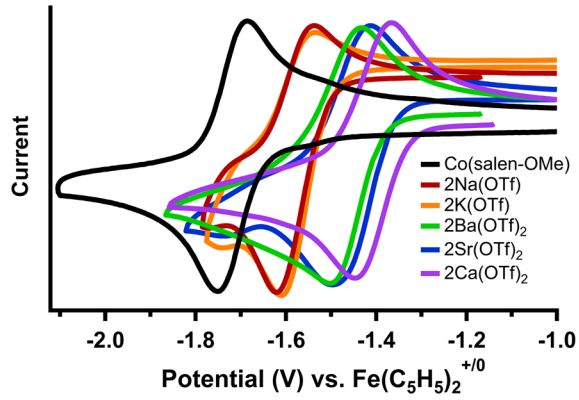

Figure 2. Cyclic voltammograms of the reversible Co(II/I) redox couples of Co(salen−OMe) and **2M** (M = Na^+, K^+, Ca^{2+}, Sr^{2+}, and Ba^{2+}) in 0.5 M tetrabutylammonium hexafluorophosphate in DMF under N_2. Individual CVs are shown in Figures S13−S18.

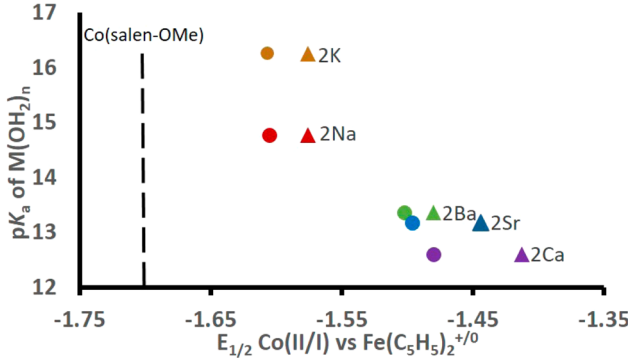

Figure 3. Experimental Co(II/I) redox potentials (circles) for **2M** vs pK_a of M(OH$_2$)$_n$. The triangles correspond to the calculated redox potential for **2M** using only the electrostatic field potential of M on the Co(II) ion and Co(salen−OMe) as the baseline redox potential.

minor changes to the cyclic voltammograms (<10 mV) were observed (S19−21).

Previous studies incorporating alkali and alkaline earth metal cations into Schiff base complexes with Cu, Ni, and Zn display anodic shifts of similar magnitudes in the reduction potential. The changes in reduction potential were attributed to inductive effects from the Lewis acid, which decreases the electron density at the metal, making them easier to reduce.[22]

Electronic and Vibrational Spectroscopy. In order to determine the magnitude of the inductive effect due to M on the ligand field of the Co(II), the compounds were examined

DOI: 10.1021/acs.inorgchem.6b03098
Inorg. Chem. 2017, 56, 3713−3718

by electronic absorption and infrared spectroscopy. The electronic absorption spectra in dimethylformamide are shown in Figures S22−S33 and are summarized in Table 1. The absorption spectrum of Co(salen−OMe) exhibits $\pi \rightarrow \pi^*$ and d $\rightarrow \pi^*$ (MLCT) transitions[23] at 360 and 415 nm, respectively. The $\pi \rightarrow \pi^*$ band is partially obscured in **2M**, but a slight red shift (≤15 nm) is observed for dicationic **2Ca(OTf)$_2$**, **2Sr(OTf)$_2$**, and **2Ba(OTf)$_2$**. The molar absorptivity for the d $\rightarrow \pi^*$ charge transfer band in **2K(OTf)** and **2Na(OTf)** is comparable to Co(salen−OMe) for this transition, while for **2Ca(OTf)$_2$**, **2Ba(OTf)$_2$**, and **2Sr(OTf)$_2$** it has significantly lowered absorptivity. Co(salen−OMe) also has an absorption at 480 nm; this peak is likely obscured in the **2M** spectra by more intense neighboring absorptions. However, the second d → d transition at 555 nm for Co(salen−OMe) is present in **2M**, with a minor red shift of 10 and 25 nm for the monocationic versus dicatonic complexes, respectively. Although the changes in the absorption spectra indicate M has some influence on the ligand field around the Co(II) ion, the overall effect appears minimal compared to the changes in redox potential.

The solid-state infrared spectra of **2M** were taken to compare the electronic environments of the cobalt center (Figures S34−S40). The vibrational frequency of the imine C═N bond for **2M** increases slightly with the Lewis acid strength of M (Table 1) and, with Co(salen−OMe), displays a linear relationship with the Co(II/I) reduction potential (Figure S41). However, the values span a small range (22 cm^{-1}), suggesting the Lewis acids have a minimal effect on the electron density of the Co(II) ion in **2M**.

Calculated Electric Field Potential. An alternative explanation for the anodic shifts in redox potential is through the electric field potential imposed by the nonredox active cation. An electrostatic effect has been cited as the source of redox potential shifts in other heterobimetallic complexes.[11,24] eq 1 describes the electric field potential (ΔE, in V) at the Co(II) ion by a point charge q (cation M), where $\in$ is the dielectric constant, and r is the distance between Co and M.

$$\Delta E = \frac{q}{4\pi \in \mathrm{r}} \quad (1)$$

Values for ΔE were calculated for **2M** using the distances between Co(II) and M in the solid-state structure as r and the dielectric constant of DMF[25] as $\in$, shown in Table 1. This simple model for calculating the electric field potential has two sources of error. The first is assuming r in **2M** is the same in solution as in the solid state; we believe this would only result in a minor deviation from our calculated values. A larger uncertainty is due to the dielectric constant between the cations; we used the value for DMF, but the medium between the Co(II) and M is more accurately described by the phenoxide ligand that bridges the two ions. However, using this approximation we see the magnitude of the electric field potential by M is consistent with the observed anodic shift. The anodic shift for the dications (2q) is also roughly double that observed for the monocations (q), consistent with an electric field effect.

An electrostatic interaction would explain the identical redox potentials observed for **2K** and **2Na**. Although there is a difference in Lewis acidity between the monocations,[21c] the distance between Co(II) and K^+ or Na^+ is nearly the same, resulting in essentially the same electrostatic potential on Co(II) (Table 1). The redox potentials of the dications trend with the Lewis acidity of M, but the Lewis acidity is also directly related to the ionic radii of M. The latter is reflected in changes in r due to the size of M.

CONCLUSIONS

On the basis of the spectroscopic studies and calculated electrostatic effect of the alkali and alkaline earth metal centers, the anodic shift in the redox potential in **2M** compared to that in Co(salen−OMe) can largely be attributed to an electrostatic field potential. An inductive effect through the bridging phenoxide ligand appears to play a smaller role.

Redox potentials of synthetic transition metal complexes are most commonly tuned by incorporating electron donating or withdrawing functionalities into the ligand. As a result, changes in the free energy for electron transfer are coupled to changes in the electron density of the redox active site. This study indicates cations in the secondary coordination sphere can adjust the redox potential without significantly affecting the electronic structure at the redox active site. The decoupling of free energy and electronic structure points to their utility in mediating redox reactivity. These results highlight how cations can contribute to tuning the potential of redox-active centers through the simple parameters of distance and charge. We are currently investigating how the shift in redox potential due to nonredox active cations affect linear free energy scaling relationships in redox catalysis.

ASSOCIATED CONTENT

Supporting Information

The Supporting Information is available free of charge on the ACS Publications website at DOI: 10.1021/acs.inorgchem.6b03098.

Experimental methods, synthetic procedures, ^{1}H and ^{13}C NMR spectra, HRMS and ESI-MS data, electrochemical data, UV−visible spectra, X-ray crystallographic data, infrared spectra (PDF)
2Na(OTf) (1513027) (CIF)
2Na(BF4) (1491801) (CIF)
2K(OTf) (1513026) (CIF)
2K(BF4) (1489650) (CIF)
2Ca(OTf)$_2$ (1491803) (CIF)
2Sr(OTf)$_2$, (1491802) (CIF)
2Ba(OTf)$_2$ (1489654) (CIF)
Co(salen-OMe) (1513025)(CIF)

AUTHOR INFORMATION

Corresponding Author

*E-mail: j.yang@uci.edu.

ORCID

Jenny Y. Yang: 0000-0002-9680-8260

Notes

The authors declare no competing financial interest.

ACKNOWLEDGMENTS

This material is based upon work supported by the National Science Foundation under Grant No. 1554744.

REFERENCES

(1) (a) Yocum, C. F. The calcium and chloride requirements of the O2 evolving complex. *Coord. Chem. Rev.* **2008**, *252* (3−4), 296−305. (b) Ferreira, K. N.; Iverson, T. M.; Maghlaoui, K.; Barber, J.; Iwata, S. Architecture of the Photosynthetic Oxygen-Evolving Center. *Science*

DOI: 10.1021/acs.inorgchem.6b03098
Inorg. Chem. 2017, 56, 3713−3718

2004, *303* (5665), 1831−1838. (c) Yano, J.; Kern, J.; Sauer, K.; Latimer, M. J.; Pushkar, Y.; Biesiadka, J.; Loll, B.; Saenger, W.; Messinger, J.; Zouni, A.; Yachandra, V. K. Where Water Is Oxidized to Dioxygen: Structure of the Photosynthetic Mn4Ca Cluster. *Science* **2006**, *314* (5800), 821−825. (d) Barber, J. Crystal Structure of the Oxygen-Evolving Complex of Photosystem II. *Inorg. Chem.* **2008**, *47* (6), 1700−1710. (e) Sauer, K.; Yano, J.; Yachandra, V. K. X-ray spectroscopy of the photosynthetic oxygen-evolving complex. *Coord. Chem. Rev.* **2008**, *252* (3−4), 318−335. (f) Umena, Y.; Kawakami, K.; Shen, J.-R.; Kamiya, N. Crystal structure of oxygen-evolving photosystem II at a resolution of 1.9[thinsp]A. *Nature* **2011**, *473* (7345), 55−60. (g) Pecoraro, V. L.; Baldwin, M. J.; Caudle, M. T.; Hsieh, W. Y.; Law, N. A. A proposal for water oxidation in photosystem II. *Pure Appl. Chem.* **1998**, *70*, 925. (h) Cady, C. W.; Crabtree, R. H.; Brudvig, G. W. Functional models for the oxygen-evolving complex of photosystem II. *Coord. Chem. Rev.* **2008**, *252* (3−4), 444−455. (i) Brudvig, G. W. Water oxidation chemistry of photosystem II. *Philos. Trans. R. Soc., B* **2008**, *363* (1494), 1211−1219. (j) Mullins, C. S.; Pecoraro, V. L. Reflections on small molecule manganese models that seek to mimic photosynthetic water oxidation chemistry. *Coord. Chem. Rev.* **2008**, *252* (3−4), 416−443.

(2) Yiu, S.-M.; Man, W.-L.; Lau, T.-C. Efficient Catalytic Oxidation of Alkanes by Lewis Acid/[OsVI(N)Cl4]− Using Peroxides as Terminal Oxidants. Evidence for a Metal-Based Active Intermediate. *J. Am. Chem. Soc.* **2008**, *130* (32), 10821−10827.

(3) (a) Miller, C. G.; Gordon-Wylie, S. W.; Horwitz, C. P.; Strazisar, S. A.; Peraino, D. K.; Clark, G. R.; Weintraub, S. T.; Collins, T. J. A Method for Driving O-Atom Transfer: Secondary Ion Binding to a Tetraamide Macrocyclic Ligand. *J. Am. Chem. Soc.* **1998**, *120* (44), 11540−11541. (b) Guo, H.; Chen, Z.; Mei, F.; Zhu, D.; Xiong, H.; Yin, G. Redox Inactive Metal Ion Promoted C-H Activation of Benzene to Phenol with PdII(bpym): Demonstrating New Strategies in Catalyst Designs. *Chem. - Asian J.* **2013**, *8* (5), 888−891. (c) Dong, L.; Wang, Y.; Lv, Y.; Chen, Z.; Mei, F.; Xiong, H.; Yin, G. Lewis-Acid-Promoted Stoichiometric and Catalytic Oxidations by Manganese Complexes Having Cross-Bridged Cyclam Ligand: A Comprehensive Study. *Inorg. Chem.* **2013**, *52* (9), 5418−5427. (d) Zhang, Z.; Coats, K. L.; Chen, Z.; Hubin, T. J.; Yin, G. Influence of Calcium(II) and Chloride on the Oxidative Reactivity of a Manganese(II) Complex of a Cross-Bridged Cyclen Ligand. *Inorg. Chem.* **2014**, *53* (22), 11937−11947. (e) Chen, Z.; Yang, L.; Choe, C.; Lv, Z.; Yin, G. Non-redox metal ion promoted oxygen transfer by a non-heme manganese catalyst. *Chem. Commun.* **2015**, *51* (10), 1874−1877. (f) Qin, S.; Dong, L.; Chen, Z.; Zhang, S.; Yin, G. Non-redox metal ions can promote Wacker-type oxidations even better than copper(ii): a new opportunity in catalyst design. *Dalton Trans.* **2015**, *44* (40), 17508−17515. (g) Zhang, S.; Chen, Z.; Qin, S.; Lou, C.; Senan, A. M.; Liao, R.-Z.; Yin, G. Non-redox metal ion promoted oxidative coupling of indoles with olefins by the palladium(ii) acetate catalyst through dioxygen activation: experimental results with DFT calculations. *Org. Biomol. Chem.* **2016**, *14* (17), 4146−4157. (h) Choe, C.; Yang, L.; Lv, Z.; Mo, W.; Chen, Z.; Li, G.; Yin, G. Redox-inactive metal ions promoted the catalytic reactivity of non-heme manganese complexes towards oxygen atom transfer. *Dalton Trans.* **2015**, *44* (19), 9182−9192. (i) Park, J.; Morimoto, Y.; Lee, Y.-M.; Nam, W.; Fukuzumi, S. Metal Ion Effect on the Switch of Mechanism from Direct Oxygen Transfer to Metal Ion-Coupled Electron Transfer in the Sulfoxidation of Thioanisoles by a Non-Heme Iron(IV)−Oxo Complex. *J. Am. Chem. Soc.* **2011**, *133* (14), 5236−5239.

(4) Cammarota, R. C.; Lu, C. C. Tuning Nickel with Lewis Acidic Group 13 Metalloligands for Catalytic Olefin Hydrogenation. *J. Am. Chem. Soc.* **2015**, *137* (39), 12486−12489.

(5) Park, Y. J.; Ziller, J. W.; Borovik, A. S. The Effects of Redox-Inactive Metal Ions on the Activation of Dioxygen: Isolation and Characterization of a Heterobimetallic Complex Containing a MnIII−(μ-OH)−CaII Core. *J. Am. Chem. Soc.* **2011**, *133* (24), 9258−9261.

(6) (a) Morimoto, Y.; Kotani, H.; Park, J.; Lee, Y.-M.; Nam, W.; Fukuzumi, S. Metal Ion-Coupled Electron Transfer of a Nonheme Oxoiron(IV) Complex: Remarkable Enhancement of Electron-Transfer Rates by Sc3+. *J. Am. Chem. Soc.* **2011**, *133* (3), 403−405. (b) Fukuzumi, S.; Morimoto, Y.; Kotani, H.; Naumov, P.; Lee, Y.-M.; Nam, W. Crystal structure of a metal ion-bound oxoiron(IV) complex and implications for biological electron transfer. *Nat. Chem.* **2010**, *2* (9), 756−759. (c) Karlin, K. D. Bioinorganic chemistry: Redox control of oxoiron(IV). *Nat. Chem.* **2010**, *2* (9), 711−712.

(7) Hong, S.; Lee, Y.-M.; Sankaralingam, M.; Vardhaman, A. K.; Park, Y. J.; Cho, K.-B.; Ogura, T.; Sarangi, R.; Fukuzumi, S.; Nam, W. A Manganese(V)−Oxo Complex: Synthesis by Dioxygen Activation and Enhancement of Its Oxidizing Power by Binding Scandium Ion. *J. Am. Chem. Soc.* **2016**, *138* (27), 8523−8532.

(8) (a) Tsui, E. Y.; Agapie, T. Reduction potentials of heterometallic manganese−oxido cubane complexes modulated by redox-inactive metals. *Proc. Natl. Acad. Sci. U. S. A.* **2013**, *110* (25), 10084−10088. (b) Tsui, E. Y.; Tran, R.; Yano, J.; Agapie, T. Redox-inactive metals modulate the reduction potential in heterometallic manganese−oxido clusters. *Nat. Chem.* **2013**, *5* (4), 293−299. (c) Krewald, V.; Neese, F.; Pantazis, D. A. Redox potential tuning by redox-inactive cations in nature's water oxidizing catalyst and synthetic analogues. *Phys. Chem. Chem. Phys.* **2016**, *18* (16), 10739−10750. (d) Lin, P.-H.; Takase, M. K.; Agapie, T. Investigations of the Effect of the Non-Manganese Metal in Heterometallic-Oxido Cluster Models of the Oxygen Evolving Complex of Photosystem II: Lanthanides as Substitutes for Calcium. *Inorg. Chem.* **2015**, *54* (1), 59−64.

(9) Herbert, D. E.; Lionetti, D.; Rittle, J.; Agapie, T. Heterometallic Triiron-Oxo/Hydroxo Clusters: Effect of Redox-Inactive Metals. *J. Am. Chem. Soc.* **2013**, *135* (51), 19075−19078.

(10) Al Obaidi, N.; Beer, P. D.; Bright, J. P.; Jones, C. J.; McCleverty, J. A.; Salam, S. S. The synthesis and electrochemistry of novel redox responsive molybdenum complexes containing cyclic polyether cation binding sites. *J. Chem. Soc., Chem. Commun.* **1986**, *3*, 239−241.

(11) (a) Plenio, H.; Diodone, R. Complexation of Na+ in Redox-Active Ferrocene Crown Ethers, a Structural Investigation, and an Unexpected Case of Li+ Selectivity. *Inorg. Chem.* **1995**, *34* (15), 3964−3972. (b) Beer, P. D.; Blackburn, C.; McAleer, J. F.; Sikanyika, H. Redox-responsive crown ethers containing a conjugated link between the ferrocene moiety and a benzo crown ether. *Inorg. Chem.* **1990**, *29* (3), 378−381. (c) Andrews, M. P.; Blackburn, C.; McAleer, J. F.; Patel, V. D. Redox-active crown ethers: transmission of cation binding to a redox centre via a conjugated link. *J. Chem. Soc., Chem. Commun.* **1987**, *14*, 1122−1124.

(12) Delgado, M.; Ziegler, J. M.; Seda, T.; Zakharov, L. N.; Gilbertson, J. D. Pyridinediimine Iron Complexes with Pendant Redox-Inactive Metals Located in the Secondary Coordination Sphere. *Inorg. Chem.* **2016**, *55* (2), 555−557.

(13) (a) Risch, M.; Klingan, K.; Ringleb, F.; Chernev, P.; Zaharieva, I.; Fischer, A.; Dau, H. Water Oxidation by Electrodeposited Cobalt Oxides—Role of Anions and Redox-Inert Cations in Structure and Function of the Amorphous Catalyst. *ChemSusChem* **2012**, *5* (3), 542−549. (b) Hadt, R. G.; Hayes, D.; Brodsky, C. N.; Ullman, A. M.; Casa, D. M.; Upton, M. H.; Nocera, D. G.; Chen, L. X. X-ray Spectroscopic Characterization of Co(IV) and Metal−Metal Interactions in Co4O4: Electronic Structure Contributions to the Formation of High-Valent States Relevant to the Oxygen Evolution Reaction. *J. Am. Chem. Soc.* **2016**, *138* (34), 11017−11030. (c) Hodel, F. H.; Luber, S. Redox-Inert Cations Enhancing Water Oxidation Activity: The Crucial Role of Flexibility. *ACS Catal.* **2016**, *6*, 6750−6761. (d) Evangelisti, F.; Moré, R.; Hodel, F.; Luber, S.; Patzke, G. R. 3d−4f {CoII3Ln(OR)4} Cubanes as Bio-Inspired Water Oxidation Catalysts. *J. Am. Chem. Soc.* **2015**, *137* (34), 11076−11084.

(14) Van Staveren, C. J.; Van Eerden, J.; Van Veggel, F. C. J. M.; Harkema, S.; Reinhoudt, D. N. Cocomplexation of neutral guests and electrophilic metal cations in synthetic macrocyclic hosts. *J. Am. Chem. Soc.* **1988**, *110* (15), 4994−5008.

(15) Shannon, R. Revised effective ionic radii and systematic studies of interatomic distances in halides and chalcogenides. *Acta Crystallogr., Sect. A: Cryst. Phys., Diffr., Theor. Gen. Crystallogr.* **1976**, *32* (5), 751−767.

DOI: 10.1021/acs.inorgchem.6b03098
Inorg. Chem. 2017, 56, 3713−3718

(16) Akine, S.; Utsuno, F.; Piao, S.; Orita, H.; Tsuzuki, S.; Nabeshima, T. Synthesis, Ion Recognition Ability, and Metal-Assisted Aggregation Behavior of Dinuclear Metallohosts Having a Bis(Saloph) Macrocyclic Ligand. *Inorg. Chem.* **2016**, *55* (2), 810−821.
(17) Liu, D.-F.; Lü, X.-Q.; Lu, R. Homogeneous and heterogeneous styrene epoxidation catalyzed by copper(II) and nickel(II) Schiff base complexes. *Transition Met. Chem.* **2014**, *39* (6), 705−712.
(18) West, B. O. Studies on bond type in certain cobalt complex compounds. Part IV. The exchange reactions of quadridentate complexes. *J. Chem. Soc.* **1954**, *0*, 395−400.
(19) Yang, L.; Powell, D. R.; Houser, R. P. Structural variation in copper(i) complexes with pyridylmethylamide ligands: structural analysis with a new four-coordinate geometry index, [small tau]4. *Dalton Trans.* **2007**, *9*, 955−964.
(20) Alleman, K. S.; Peters, D. G. Catalytic reduction of iodoethane by cobalt(I) salen electrogenerated at vitreous carbon cathodes. *J. Electroanal. Chem.* **1998**, *451* (1−2), 121−128.
(21) (a) Harned, H. S.; Geary, C. G. The Ionic Activity Coefficient Product and Ionization of Water in Barium Chloride Solutions from 0 to 50°. *J. Am. Chem. Soc.* **1937**, *59* (10), 2032−2035. (b) Kangro, W. Konzentrierte wäßrige Lösungen, II. *Z. Phys. Chem.* **1962**, *32*, 273. (c) The Lewis acidity for all cations used in this study have not been experimentally quantified using a single method. The values for Na^+, Ca^{2+}, Sr^{2+}, and Ba^{2+} used in Table 1 correspond to the pK_b of the aquated hydroxide species (ref 21b), measured electrometrically in cells containing Ag/AgCl with hydrogen electrodes. The value for K^+ was calculated using the dissociation energy of water through vapor pressure measurements (ref 21a). As a result, it is uncertain whether the relative pK_b value for K^+ is comparable to that of the other cations. However, we expect Na^+ to be more Lewis acidic than K^+ based on the equivalent charge and the smaller ionic radii of the former.
(22) (a) Van Veggel, F. C. J. M.; Harkema, S.; Bos, M.; Verboom, W.; Van Staveren, C. J.; Gerritsma, G. J.; Reinhoudt, D. N. Metallomacrocycles: synthesis, x-ray structure, electrochemistry, and ESR spectroscopy of mononuclear and heterodinuclear complexes. *Inorg. Chem.* **1989**, *28* (6), 1133−1148. (b) Van Veggel, F. C. J. M.; Harkema, S.; Bos, M.; Verboom, W.; Woolthuis, G. K.; Reinhoudt, D. N. Incorporation of nitrogen-oxygen bonds in metallomacrocycles. Synthesis, x-ray structure, and electrochemistry of heterodinuclear complexes. *J. Org. Chem.* **1989**, *54* (10), 2351−2359.
(23) (a) Pui, A.; Policar, C.; Mahy, J.-P. Electronic and steric effects in cobalt Schiff bases complexes: Synthesis, characterization and catalytic activity of some cobalt(II) tetra-halogens-dimethyl salen complexes. *Inorg. Chim. Acta* **2007**, *360* (6), 2139−2144. (b) Ortiz, B.; Park, S.-M. Electrochemical and spectroelectrochemical studies of cobalt salen and salophen as oxygen reduction catalysts. *Bull. Korean Chem. Soc.* **2000**, *21* (4), 405−411.
(24) (a) Horwitz, C. P.; Ciringh, Y. Synthesis and electrochemical properties of oxo-bridged manganese dimers incorporating alkali and alkaline earth cations. *Inorg. Chim. Acta* **1994**, *225* (1−2), 191−200. (b) Serr, B. R.; Andersen, K. A.; Elliott, C. M.; Anderson, O. P. A triply-bridged dinuclear tris(bipyridine)iron(II) complex: synthesis and electrochemical and structural studies. *Inorg. Chem.* **1988**, *27* (24), 4499−4504.
(25) Multiplied by the permittivity of free space.

DOI: 10.1021/acs.inorgchem.6b03098
Inorg. Chem. 2017, 56, 3713−3718